NASA TECHNICAL MEMORANDUM

NASA TM X-71640

NASA TM X-71640

(NASA-TM-X-71640) LIQUID JET PUMPED BY RISING GAS BUBBLES (NASA) 9 p HC $3.25 CSCL 20D

N75-14997

Unclas
G3/34 07766

LIQUID JET PUMPED BY RISING GAS BUBBLES

by Nihad A. Hussain* and Robert Siegel
Lewis Research Center
Cleveland, Ohio 44135

TECHNICAL PAPER to be presented at
Fluids Engineering Conference sponsored by the
American Society of Mechanical Engineers
Minneapolis, Minnesota, May 5-7, 1975

*Summer faculty fellow from
California State University
San Diego, California 92115

ABSTRACT

From observations of a stream of gas bubbles rising through a liquid, a two-phase mathematical model is proposed for calculating the induced turbulent vertical liquid flow. The bubbles provide a large buoyancy force and the associated drag on the liquid moves the liquid upward. The liquid pumped upward consists of the bubble wakes and the liquid brought into the jet region by turbulent entrainment. The expansion of the gas bubbles as they rise through the liquid is taken into account. The continuity and momentum equations are solved numerically for an axisymmetric air jet submerged in water. Water pumping rates are obtained as a function of air flow rate and depth of submergence. Comparisons are made with limited experimental information in the literature.

NOMENCLATURE

a local outer radius of liquid jet region

a_c local radius of bubbly core region

E_o turbulent jet entrainment coefficient

g acceleration of gravity

K ratio of bubble wake volume to bubble volume

L depth of jet origin below liquid surface

M mass flow rate

p pressure

p_a atmospheric pressure

Q volume flow rate

r radial coordinate, origin is at jet axis

R perfect gas constant

T absolute temperature

u velocity in x direction

u_∞ terminal velocity of single bubble rising in infinite liquid region

v velocity in radial direction

x vertical coordinate along jet axis, origin is at gas release orifice

ρ fluid density

σ surface tension

Subscripts:

c jet core region

g gas phase

i,o inside and outside of a particular jet region

l liquid phase

INTRODUCTION

Liquid pumping can be obtained by utilizing the buoyant force of gas bubbles rising through the liquid as shown in fig. 1. This is a free convection type of process using two immiscible fluids that have a large difference in density (1) (2). Because of the large density difference made possible by using a gas and a liquid, large amounts of liquid pumping can be obtained. The large local density difference is in contrast to ordinary thermally driven single phase free convection where the density variations are usually small.

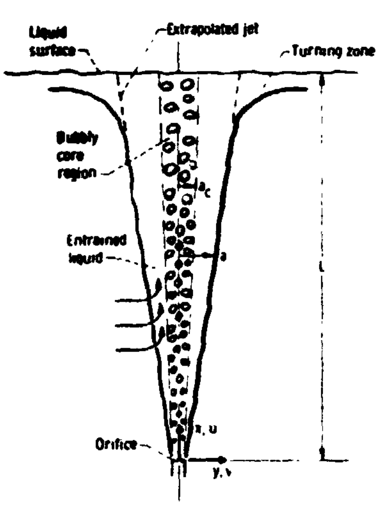

Figure 1. - Configuration of liquid jet induced by rising column of gas bubbles.

---

*Summer Faculty Fellow, NASA Lewis Research Center.

An interesting application of bubble pumping is for ice prevention in lakes (3) (4) (5). Since the maximum density of water is at 4° C, the water in the bottom regions of a quiescent lake can be as much as 4° C warmer than the surface regions when the air temperature is below freezing. Ice formation on the lake can be diminished or prevented by pumping the warmer bottom water toward the surface by means of rising air bubbles. Bubble pumping is also used in fluidized beds, and for aeration in water purification and waste treatment plants. The flow induced by a curtain of rising air bubbles has also been considered as a breakwater for oncoming water waves (1) (5).

The purpose of this paper is to formulate a two-phase model and analyze the turbulent liquid pumping by a rising discharge of gas bubbles. By means of the drag on the liquid, the buoyancy force of the bubbles imparts an upward momentum to the liquid. There is turbulent entrainment of liquid into the rising jet as indicated in fig. 1, and the result is that substantial vertical liquid pumping can result. The extent of the pumping is illustrated by experimental results in refs. (4) and (5) which show that for bubbles rising through 1.68 m (5.5 ft) of water, an air flow of 0.000472 m^3/sec (1/60 ft^3/sec) produced a pumped liquid volume 120 times that of the gas. In ref. (6) the volume of water pumped per unit volume of air for an orifice at a depth of 4.5 m (14.7 ft) varied from about 60 to 175 depending on the air flow rate. The analysis given here will provide the liquid pumping rate as a function of bubble rise distance and gas flow rate.

Experimental measurements of a rising water jet pumped by air were made by Kobus (6) at several air flow rates for an orifice depth of 4.5 m. A theory was given utilizing the experimentally measured flow to specify the entrainment term in the continuity equation. In ref. (7) an analysis was made of the bubble pumped jet in a manner analogous to a turbulent convective plume such as in ref. (8). This procedure leads to a singularity where the fluid velocity becomes infinite at the jet origin, making it necessary to define an apparent origin in order to compare the analytical results with experiment. The data of Kobus (6) was used in ref. (7) to determine the coefficients governing the flow such as the jet spreading rate and the turbulent entrainment coefficient. In order to obtain better agreement between the analysis and the experiment of Kobus, it was found necessary to decrease the entrainment coefficient substantially as the air flow decreased.

In ref. (9) analytical expressions are given from an approximate analysis by I. M. Konovalov of the water pumped by air released from a submerged perforated pipe. The present situation is axisymmetric, whereas the perforated pipe provides a jet that is two dimensional in rectangular coordinates. The empirical constants in the theory were evaluated from laboratory observations for depths of the perforated pipe up to about 1 m and for air flow rates up to about 0.00139 m^3/sec per meter of pipe length. Some limited full scale tests were also made at depths up to 10 m. Some data for a two-dimensional plume are also given in ref. (6). The analysis here is concerned with localized discharges spaced apart along the length of a submerged pipe; hence an axisymmetric jet is being considered rather than the perforated pipe.

The present work is an attempt to model the gas driven jet as a two-phase flow. A simplified two-phase model is constructed consisting of a bubbly core and an outer liquid flow. An entrainment model is constructed to account for the contributions to the entrainment by the outer liquid flow, the bubble wakes, and the rising gas bubbles.

ANALYSIS

Model Description

A glass tube having an opening about 1-1/2 mm in diameter was placed at the bottom of a tank 0.6 m deep and 0.31 m square in horizontal cross section. Motion pictures were made at several rates of air flow from the tube, and typical configurations of rising bubbles are shown in fig. 2.[1] Based on these observations, a model was constructed which was a compromise between mathematical difficulty and physical realism. In the model, as shown in fig. 3, the jet is considered axisymmetrical with two regions. There is a central core surrounding the jet axis consisting of large bubbles rising in a chain bubble fashion and separated by liquid wakes that are carried along by the bubbles. Surrounding the core is an outer region of entrained

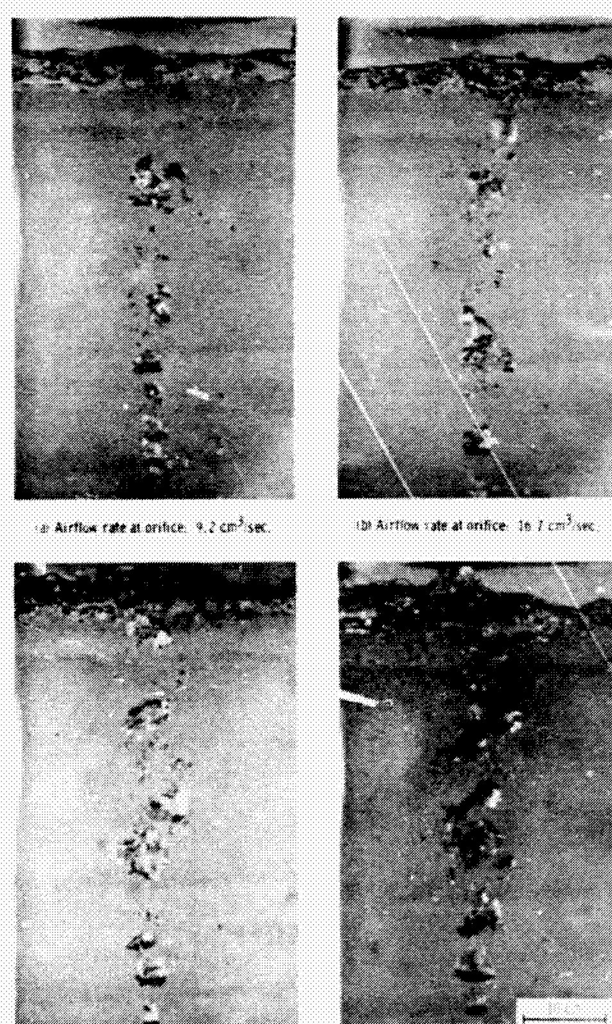

(a) Airflow rate at orifice: 9.2 cm³/sec.

(b) Airflow rate at orifice: 16.7 cm³/sec.

(c) Airflow rate at orifice: 29.2 cm³/sec.

(d) Airflow rate at orifice: 42.5 cm³/sec.

Figure 2. - Air bubble rise patterns from 1 1/2 mm diameter orifice in water tank 0.6 m deep with 0.31 m square cross section (obtained by Y. Y. Hsu and N. A. Hussaini).

[1] Experimental results obtained with help of Dr. Y. Y. Hsu.

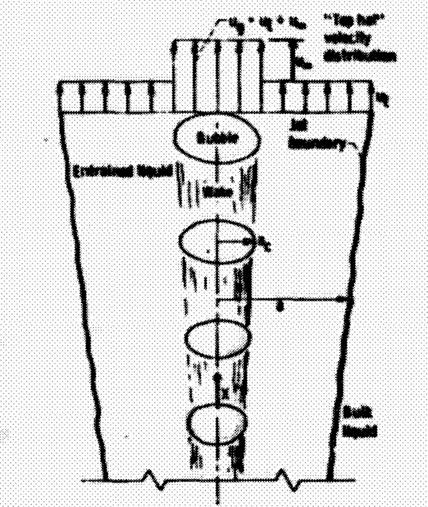

Figure 3. - Mathematical model of liquid jet induced by rising column of gas bubbles.

liquid being carried upward by the drag on the liquid arising from the buoyancy force of the bubbles. This model permits using different relations for the entrainment by the gas and by the liquid regions.

The flow field is assumed to be steady, isothermal and fully turbulent. The liquid density is assumed constant, but the gas density varies with the local pressure in accordance with the perfect gas law; thus the bubbles expand as they rise through the liquid. The bubbles are assumed to be sufficiently large that their drag is fully turbulent and hence they rise at a constant terminal velocity relative to the liquid. The local bubble velocity is assumed equal to the local liquid velocity plus the bubble terminal velocity. It is assumed that the gas leaves the orifice with negligible upward momentum. After the gas is released, there is an adjustment region within which the bubbles achieve their terminal velocity. For an installation in a lake or river this region would be small compared with the total rise height and hence this region is not taken into account.

As shown in fig. 1 the rising jet flow will turn at the liquid surface and move radially outward. At the surface the vertical velocity component has to go to zero. However, to incorporate this condition requires coupling the solutions for the jet and the turning zone which is a difficult analysis. The turning zone is not accounted for here; it is assumed that the jet continues to the surface as shown by the dotted extrapolation lines in fig. 1. Because of their strong vertical buoyancy force, the bubbles do not turn very much with the flow; hence they exert their pumping effect all the way to the surface. Also there is zero shear at the liquid surface which facilitates the turning and tends to minimize the influence of the turning zone in the rising plume. These same types of assumptions are discussed in ref. (10) for a free convection plume above a heated cylinder. Consequently an analysis without the effect of the turning zone should yield reasonable vertical pumping rates.

Gas Continuity

For a single rising bubble, let the ratio of the wake volume to the bubble volume be a quantity K. From ref. (11), for bubble Reynolds numbers greater than about 200, which would be reasonable for the large bubbles in the present application, the K is essentially constant and equals about 1.5. Then in the core region of local radius $a_c(x)$ in fig. 3, on the average $1/(K+1)$ of the vertical height is occupied by gas bubbles and $K/(K+1)$ is occupied by wake regions. This assumes for mathematical simplicity that the bubbles are rising in a chain-bubble fashion in which the bubbles are vertically spaced by the liquid wakes. Strictly speaking such a configuration exists only over a certain range of flow rates. However, the results from this model may apply to other bubble regimes. This is because, as discussed later, the turbulent entrainment of liquid by gas is minor compared with the entrainment by liquid. This tends to diminish the importance of the exact configuration of the rising gas. Since the gas weight flow rate is constant,

$$M_g = \int_0^{a_c} \frac{2\pi r}{K+1} \rho_g u_g \, dr = \text{constant} \qquad (1)$$

Perfect Gas Law

The pressure at height x above the nozzle is $\rho_l(L - x)$. Then from the perfect gas law the gas density at x is

$$\rho_g = \frac{1}{RT}\left[p_a + \rho_l(L - x)\right] \qquad (2)$$

where p_a is atmospheric pressure at the liquid surface.

Liquid Continuity

The liquid continuity equation accounts for the liquid carried into the jet by turbulent entrainment. The entrained liquid goes into the liquid region surrounding the core, or into the bubble wakes which are growing as the rising bubbles expand,

$$\frac{d}{dx}\left[\frac{K}{K+1}\int_0^{a_c} 2\pi r\rho_l u_g \, dr + \int_{a_c}^{\infty} 2\pi r\rho_l u_l \, dr\right] = -(2\pi\rho_l r v)_{r\to\infty} \qquad (3)$$

The term on the right will be expressed later in terms of a turbulent entrainment relation.

Gas and Liquid Momentum

In most applications involving air driven jets, the surrounding body of water is large; hence for simplicity in the present analysis, the surrounding liquid region will be assumed infinite. The analysis of a jet in a small container would be much more complicated because of liquid recirculation and the interaction with the container walls.

The upward buoyancy force of the bubbles produces a change in momentum (usually quite small) of the gas bubbles, a momentum change of the liquid in the bubble wakes, and a momentum change of the liquid in the region surrounding the bubbly core. This yields the momentum equation as,

$$\int_0^{a_c} \frac{g}{K+1}(\rho_l - \rho_g)2\pi r \, dr = \frac{d}{dx}\left[\int_0^{a_c} \frac{1}{K+1} 2\pi r\rho_g u_g^2 \, dr + \int_0^{a_c} \frac{K}{K+1} 2\pi r\rho_l u_g^2 \, dr + \int_{a_c}^{\infty} 2\pi r\rho_l u_l^2 \, dr\right] \qquad (4)$$

"Top Hat" Distributions

To integrate eqs. (1), (3), and (4), "top hat" velocity profiles are assumed which have yielded good results for free convection plumes (8),

$$u_g(x,r) = u_g(x) \quad 0 \le r \le a_c(x) \tag{5a}$$

$$u_l(x,r) = \begin{cases} u_l(x) & a_c(x) < r \le a(x) \\ 0 & a(x) < r \end{cases} \tag{5b}$$

The u_g and u_l are related by

$$u_g(x) = u_l(x) + u_\infty \tag{6}$$

where u_∞ is the terminal velocity of a single bubble rising in a large region of quiescent liquid.

Insert eq. (5) into eqs. (1), (3), and (4) to obtain

$$M_g = \frac{\pi a_c^2}{K+1} \rho_g u_g = \text{constant} \tag{7}$$

$$\frac{\pi K \rho_l}{K+1} \frac{d}{dx}\left(u_g a_c^2\right) + \pi\rho_l \frac{d}{dx}\left[\left(a^2 - a_c^2\right)u_l\right] = -\left(2\pi\rho_l r v\right)_{r\to\infty} \tag{8}$$

$$\frac{\pi K \rho_l}{K+1} \frac{d}{dx}\left(u_g^2 a_c^2\right) + \pi\rho_l \frac{d}{dx}\left[u_l^2\left(a^2 - a_c^2\right)\right] + \frac{\pi}{K+1}\frac{d}{dx}\left(\rho_g u_g^2 a_c^2\right) = \frac{\pi g}{K+1}\left(\rho_l - \rho_g\right) a_c^2 \tag{9}$$

Entrainment Function

An expression is now needed for the entrainment on the right side of eq. (8). As discussed by Morton (12) for free convection plumes above fires, for a buoyant single phase jet the entrainment depends on an additional variable which is the density in the plume relative to the density of the surrounding fluid. The entrainment is reduced when the plume density is smaller than the density of the surrounding fluid. The present situation involves two distinct phases that each maintain their separate identities; hence there will be two types of entrainment, liquid-liquid and gas-liquid. For the latter there is a lack of entrainment information when the density ratio is as small as that for air to water. As soon as some liquid is in motion, much of the entrainment is by liquid entraining additional liquid which is reasonably well understood.

It was deduced in ref. (12) by using the information in ref. (13), that for a single phase jet the usual jet entrainment coefficient E_o used when the jet and outer fluid have the same density, should be modified when the jet and outer fluid densities are different. The E_o is multiplied by the density ratio $(\rho_i/\rho_o)^{1/2}$ where ρ_i is the density in the jet and ρ_o is outside the jet. For the present situation the liquid-liquid entrainment terms will therefore have a unity ratio factor, while the gas-liquid terms will contain $(\rho_g/\rho_l)^{1/2}$. Since the entrainment is so different for the two phases, the two-phase nature of the jet will be retained rather than trying to assign an average density to the entire jet.

The entrainment also depends on the velocity of the jet relative to its surroundings, and on the interfacial area between the jet and the surrounding region. These velocities and areas are different for the gas and liquid portions. The liquid region moving at velocity u_l as shown in fig. 3, entrains liquid from the quiescent fluid around it. The higher velocity bubbly region is moving at velocity u_∞ relative to its surrounding liquid, and hence should enhance the entrainment process. A well defined interfacial area bounding the bubbly region can only be obtained by utilizing a simplified model such as in fig. 3, and this area is used to obtain the magnitude of the entrainment. However, if this entrainment were assumed to be retained in the core, the core would then become a liquid jet containing a bubbly core and the difficulty of defining the entrainment for this two-phase inner jet would become the same as that for the original two-phase problem. Although the concept of a bubbly core is used to provide a well defined interfacial area, it is realized that the bubbly motion is actually more random. With these considerations in mind and in the absence of any better information on such a two-stage entrainment process, it is assumed that the vigorous action of the bubbly region increases the turbulence in the liquid surrounding the bubbles and thereby enhances the total entrainment into the moving region. This is in accord with the results in ref. (13) that the entrainment is a function of the excess momentum flux in the jet. Thus in the present model, as the jet grows with increasing height above the source of gas the core will retain its identity as being composed of only bubbles and their wakes. Hence the total entrainment will be taken as the entrainment by the moving liquid outside the bubbly core, augmented by the entrainment effects of the liquid wakes and gas within the core, and is given by

$$-\left(2\pi\rho_l r v\right)_{r\to\infty} = 2\pi E_o \rho_l a u_l + 2\pi E_o \rho_l \frac{K}{1+K} a_c u_\infty + 2\pi E_o \rho_l \left(\frac{\rho_g}{\rho_l}\right)^{1/2} \frac{a_c}{1+K} u_\infty \tag{10}$$

Solution for u_l and a

To obtain the amount of liquid being pumped by the rising gas, the liquid velocity and jet radius must be obtained. The liquid mass flow rate in the wake regions is known from the specified gas flow rate as $KM_g(\rho_l/\rho_g)$. The mass flow rate of liquid is then

$$M_l = \pi\left(a^2 - a_c^2\right)\rho_l u_l + KM_g \frac{\rho_l}{\rho_g} \tag{11}$$

Since M_g in eq. (7) is a constant, eqs. (8) and (9) can be simplified by using eq. (7) to eliminate some of the u_g. Eq. (10) is then substituted for the right side of eq. (8). The result is the continuity and momentum equations in the form,

$$\frac{K}{\pi} M_g \frac{d}{dx}\left(\frac{1}{\rho_g}\right) + \frac{d}{dx}\left[\left(a^2 - a_c^2\right)u_l\right] = 2E_o\left[a u_l + \frac{K a_c}{1+K} u_\infty + \left(\frac{\rho_g}{\rho_l}\right)^{1/2} \frac{a_c}{1+K} u_\infty\right] \tag{12}$$

$$K\frac{M_g}{\pi}\frac{d}{dx}\left(\frac{u_g}{\rho_g}\right)+\frac{d}{dx}\left[u_l^2\left(a^2-a_c^2\right)\right]+\frac{M_g}{\pi\rho_l}\frac{du_g}{dx}$$

$$=\frac{ga_c^2}{1+K}\left(1-\frac{\rho_g}{\rho_l}\right) \qquad (13)$$

The u_g can be eliminated in terms of u_l by using eq. (6), and the ρ_∞ is given in terms of x by eq. (2). From eq. (7) the a_c can then be eliminated in terms of u_g and x. Thus eqs. (12) and (13) are reduced to equations for the unknown $u_l(x)$ and $a(x)$. To obtain numerical results the differentiations were carried out analytically and then the equations combined to eliminate du_l/dx or da/dx. The result was the following set of simultaneous differential equations that were solved by the Runge-Kutta method (14),

$$\frac{du_l}{dx}=\left[2E_o u_\infty u_l\left\{\frac{\pi a\rho_g u_l}{M_g u_\infty}+\left[\frac{\pi\rho_g}{M_g(K+1)(u_l+u_\infty)}\right]^{1/2}\right.\right.$$

$$\left.\left.\times\left[K+\left(\frac{\rho_g}{\rho_l}\right)^{1/2}\right]\right\}-\frac{g\left(1-\frac{\rho_g}{\rho_l}\right)}{u_l+u_\infty}+\frac{K}{RT}\frac{\rho_l u_\infty}{\rho_g}\right]\Bigg/\left[\frac{(K+1)u_l}{u_l+u_\infty}\right.$$

$$\left.-\frac{\pi\rho_g a^2 u_l}{M_g}-\left(\frac{\rho_g}{\rho_l}+K\right)\right]=F(u_l,a,x) \qquad (14)$$

$$\frac{da}{dx}=E_o\left\{1+\frac{u_\infty}{au_l}\left[\frac{M_g}{\pi(K+1)\rho_g(u_l+u_\infty)}\right]^{1/2}\left[K+\left(\frac{\rho_g}{\rho_l}\right)^{1/2}\right]\right\}$$

$$+\frac{M_g\rho_l}{2\pi RT\rho_g^2 a}\left(\frac{K+1}{u_l+u_\infty}-\frac{K}{u_l}\right)$$

$$-\left[\frac{a}{2u_l}-\frac{(K+1)u_\infty M_g}{2au_l\pi\rho_g(u_l+u_\infty)^2}\right]F(u_l,a,x) \qquad (15)$$

At $x=0$, $a=a_c$, and $u_l=0$ so that $u_g=u_\infty$. Then the initial conditions at $x=0$ to begin the integration are from eq. (7),

$$a(x=0)=\left[\frac{M_g(1+K)}{\pi u_\infty\dfrac{(p_a+\rho_l L)}{RT}}\right]^{1/2}$$

and $u_l(0)=0$. The latter condition however causes starting difficulty in the integration since it is in the denominator of a few terms, so a small value was used, $u_l(0)=0.001$. The calculations were tested using smaller $u_l(0)$ and no significant changes were found.

RESULTS

To compute the induced liquid flow, a number of quantities must be specified. The results that follow are with regard to the prevention of ice in lakes by raising warm bottom water to the surface. For these conditions the bulk water is a few degrees K above freezing so in what follows T = 275 K (495° R). The terminal velocity u_∞ of a single bubble in undisturbed fluid was obtained from the relation (15) (16)

$$u_\infty=1.53\left[\frac{\sigma g(\rho_l-\rho_g)}{\rho_l^2}\right]^{1/4} \qquad (16)$$

which yielded $u_\infty=0.252$ m/sec (0.825 ft/sec) for air bubbles in water.

A significant source of uncertainty is in specifying the entrainment coefficient E_o. In ref. (17) which is concerned with the penetration of a condensing vapor jet into a liquid, a "top hat" velocity profile is used and a range of E_o from 0.06 to 0.12 is given as being found in the literature. For entrainment of various gas jets in still air with density ratios in the range $\rho_1/\rho_o=0.66$ to 14.5, the work in ref. (13) yielded $E_o=0.08$ based on considerations of the excess momentum in the jet. The entrainment is proportional to a characteristic velocity in the jet. If a Gaussian velocity profile is used, the centerline velocity is used as the characteristic velocity which is larger than the average velocity used in the "top hat" profile. As a result in ref. (18) $E_o=0.082$ is recommended for use with a Gaussian profile and $E_o=0.116$ for a "top hat" profile. In view of all these considerations it was decided to obtain two sets of calculations using $E_o=0.08$ and 0.116. The results will be discussed in the next section.

Equations (14) and (15) were integrated to $x=L$, the surface of the water, to obtain $u_l(L)$ and $a(L)$. By using eqs. (6) and (7) $a_c(L)$ is found and the upward flow of liquid then obtained from eq. (11). In reality the upward flow will begin to turn as it approaches the surface, but the influence of the water surface was not accounted for here, as previously discussed. Figure 4 gives the mass flow rate of liquid being pumped to the surface as a function of the mass flow rate of air, for the air being introduced at various depths below the surface. In terms of the same quantities fig. 5 shows the radius of the jet region at $x=L$ and fig. 6 gives the liquid velocity at $x=L$. Some of the results in fig. 5 have been cross plotted in fig. 7 to show the trend of the jet radius with orifice depth for fixed gas mass flow rates.

DISCUSSION

As shown by fig. 4 the liquid pumped to the surface increases with the depth of the orifice below the surface and with the gas flow rate. For a fixed weight flow rate, the volume of the gas introduced at the orifice decreases as the orifice depth increases. Hence it seems better to present the results in terms of gas weight flow rate than in terms of volume flow. For each orifice depth the results in fig. 4 lie fairly well along a straight line on a log-log plot. The slope decreases somewhat as L is increased but the results vary essentially as $M_l \propto M_g^{.4}$. A cross plot of the results shows that for a given M_g the M_l variation with L is also as a power function.

$M_l \propto L^{1.4}$. Then an approximate correlation of the calculated results is given by

$$M_l = C\, M_g^{.4} L^{1.4} \qquad (17)$$

When M_l and M_g are in kg/sec and L is in m, then $C = 365$ for $E_o = 0.08$ and $C = 550$ for $E_o = 0.116$. When M_l and M_g are in #/sec and L is in ft, then $C = 111$ for $E_o = 0.08$ and $C = 172$ for $E_o = 0.116$.

To examine in more detail the effect of the various entrainment terms in eq. (10) calculations were made with either the liquid wake term and/or the gas

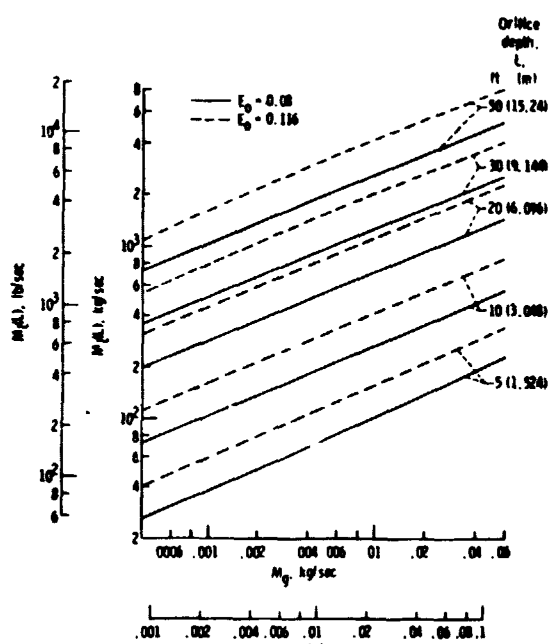

Figure 4. - Water pumping rate to surface as a function of air flow rate and orifice depth.

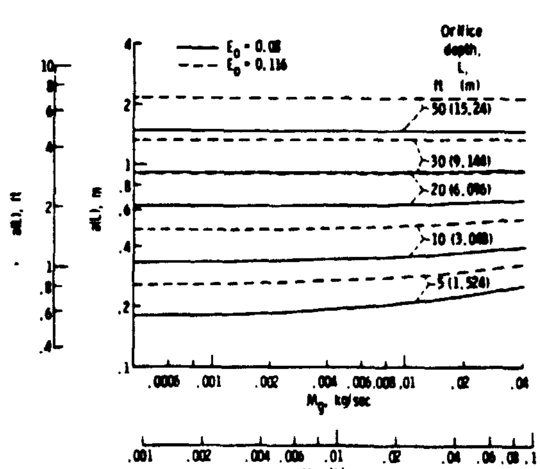

Figure 5. - Radius of rising jet at water surface as a function of air flow rate and orifice depth.

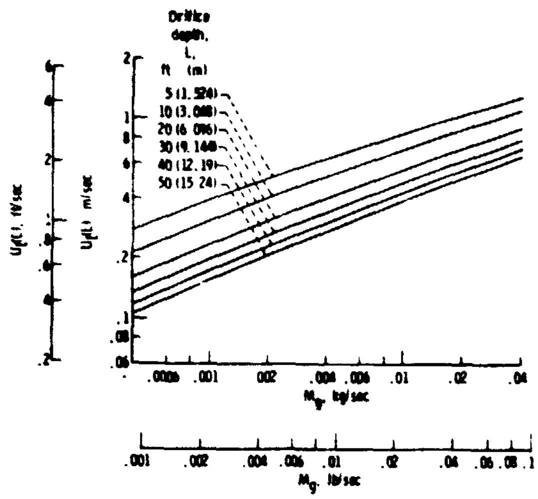

(a) Entrainment coefficient, $E_o = 0.08$.

Figure 6. - Vertical velocity of entrained liquid in rising jet at water surface.

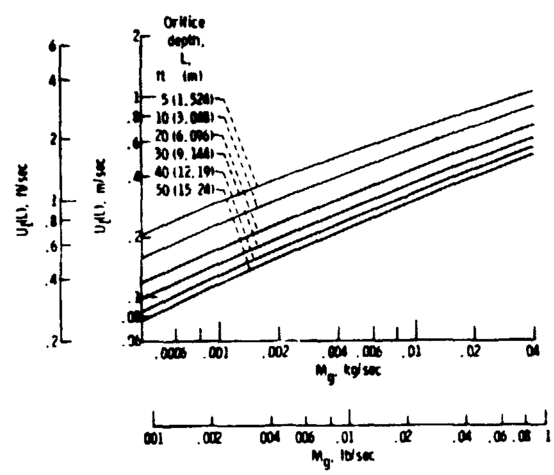

(b) Entrainment coefficient, $E_o = 0.116$.

Figure 6. - Concluded.

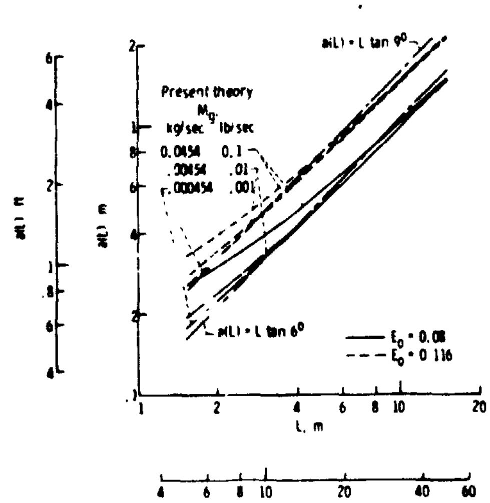

Figure 7. - Jet radius at liquid surface compared with present results and results from ref. 19.

entrainment term omitted. As might be expected because of the small value of $(\rho_g/\rho_l)^{1/2}$ the gas entrainment term had less than a 1% effect on the pumped liquid mass. The liquid wake term had a significant effect for small x where the total liquid flow is small, as it helped initiate the entrainment process. The effect of this term decreased as the total entrained flow became more substantial. For a depth of 1.524 m (5 ft) this term increased the flow in the range of 10 to 7% as the gas flow ranged from the smallest to the largest values on fig. 4. For a depth of 9.144 m (30 ft) the wake term contributed about 5% to the pumped flow for any gas flow rate.

The liquid wake term on the left side of eq. (9) is an especially important feature of the present analysis. For small x it provides inertia within the flow when the total entrained liquid is still small and prevents the buoyancy force from producing unrealistically high liquid velocities near the origin of the numerical calculations.

The bubble pumping process provides a fluctuating flow so that experimental measurements are difficult. Some comparisons will now be made with the small amount of data available in the literature. These results will serve to emphasize that although there is still appreciable uncertainty in the amount of flow being pumped, the trends with depth and gas flow rate have been approximately established. The most striking feature is that the ratio of pumped liquid volume to gas volume is quite large.

In fig. 13 of ref. (6) Kobus gives the ratio of pumped liquid volume to the gas flow rate for various gas flow rates. There is a set of data for the local flow rate at a location 3.3 m above an orifice 4.5 m deep. These local flow rates were also obtained from the present computer calculations and a comparison is made in table I. For $E_o = 0.8$, the present theory predicts a flow that is somewhat low at the high gas flow rates and somewhat high at the low flow rates. For $E_o = 0.116$ the agreement is good at the high air flow rates. Before further discussion the results of ref. (4) should be included.

In ref. (4) the following correlation is given from available data in terms of volume flow rates of air and water and depth of submergence (in ref. (5) the exponent on Q_g is 1/2),

$$Q = \text{Const. } Q_g^{2/3} L^{3/2} \tag{18}$$

Also in refs. (4) and (5) a discharge of 0.000472 m^3/sec (0.0167 ft^3/sec) of air at a submergence of 1.68 m (5.5 ft) is reported to raise about 0.0567 m^3/sec (2 ft^3/sec) of water to the surface. The present calculation yields a pumping of about 0.0373 m^3/sec (1.33 ft^3/sec) of water when $E_o = 0.08$ is used, and 0.0585 m^3/sec (2.07 ft^3/sec) when $E_o = 0.116$. The experimental values were inserted into eq. (18) to evaluate the constant and the formula then used to calculate local values for the conditions in table I. The flow rates are seen to be about twice those given in ref. (6).

It is noted from table I that the pumped volume of water per unit volume of air decreases as the air flow rate increases, so that a more efficient pumping system is obtained at low flow rates. In ref. (6) it was found that the volume pumping rate decreased as the air flow to the -0.4 power, in ref. (4) it is the -0.33 power, in ref. (5) it is the 0.5 power and the present eq. (17) gives approximately the -0.6 power. It is felt that additional sets of data are needed before refinements can be made in the theory.

To provide a little more information on bubble pumping consider briefly some results reported in ref. (9) from an approximate analysis made in 1946 by Konovalov of the pumping in a geometry that is two dimensional in rectangular coordinates as produced by air released from a submerged perforated pipe. The empirical constants in the theory were evaluated from laboratory observations for depths of the perforated pipe up to about 1 m and air flow rates up to 0.00138 m^3/sec per meter of pipe length. There were also some limited full scale tests run at depths up to 10 m. The results for orifice depths greater than 1 m are given by the correlation

$$Q_l = 0.75 \left[(10 + L)L^2 \ln\left(1 + \frac{L}{10}\right)\right]^{1/3} Q_g^{1/3} \tag{19}$$

where Q_l and Q_g are in m^3/sec and L is in meters. Because of the difference in geometry precise comparisons cannot be made, but it is interesting to see how the predictions of liquid volume pumped per unit gas volume Q_l/Q_g compare for the release from an orifice as obtained from eq. (17), and from a meter length of perforated pipe, eq. (19). Results are given in table II and it is seen that the pumping rates are of the same magnitude. The Q_g was assumed to be at the discharge location, although this was not clearly specified in the reference.

In ref. (19) it is mentioned that the bubbly region of the axisymmetric jet is approximately contained within a cone having a total included angle of 12°. Although the present mathematical model considers all the gas to be in the form of large bubbles contained in the core of the jet, in the physical case there are small bubbles that break off from the large ones as shown in fig. 2. The turbulent motion diffuses the small bubbles within the flow so that they probably extend throughout most of the entrained region. Hence the total bubbly region should give an indication of the extent of the jet region. Using a total included cone angle of 12°, the jet radius at the surface is

$$a\,(x = L) = L \tan 6^\circ = 0.105\,L \tag{20}$$

The photographs in fig. 2 indicate an increase of cone angle with gas flow rate. In fig. 2(a) the cone angle is about 14°, while in fig. 2(d) it is about 19°. Equation (20) is plotted in fig. 7 and compares reasonably well with calculated results for an entrainment coefficient of $E_o = 0.08$. For a larger total included angle of say 18°, which is characteristic of figs. 2(c) and (d), eq. (20) becomes $a(L) = 0.158\,L$. As shown by fig. 7, this provides reasonable agreement with the values computed with $E_o = 0.116$.

CONCLUSIONS

A tractable mathematical model was formulated for computing the liquid carried upward in an axisymmetric jet driven by a rising stream of gas bubbles. The model geometry was based on observations of air rising through water 0.6 m deep. Liquid is carried into the jet by turbulent entrainment and a difficulty in the analysis is in specifying the proper value of the entrainment coefficient. Calculations were made for two values of the entrainment coefficient within the range given in the literature. The large buoyancy resulting from the large density difference between the gas and liquid produced considerable liquid movement compared with ordinary liquid free convection induced by thermal means, where density differences are usually on the order of a few percent. The present results indicated that for air rising through water the rate of liquid transport to the water surface varies as the 0.4 power of the air mass flow rate and the 1.4 power of the submergence depth of the air orifice. More experimental data is needed before the theory can be further refined.

REFERENCES

1. Batchelor, G. K. "Heat Convection and Buoyancy Effects in Fluids," Quarterly Journal Royal Meteorological Society, Vol. 80, 1954, pp. 339-358.
2. DeNevers, N., "Bubble Driven Fluid Circulations," AIChE Journal Vol. 14, No. 2, Mar. 1968, pp. 222-226.
3. Williams, G. P., "Winter Water Temperatures and Ice Prevention by Air Bubbling." The Engineering Journal, Vol. 44, No. 3, March 1961, pp. 79-84.
4. Baines, W., "The Principles of Operation of Bubbling Systems." in: Proceedings Symposium on Air Bubbling, Ottawa, May 1961, National Research Council (Canada), pp. 12-22. (Available as Tech. Memo. No. 70).
5. Baines, W. D., and Hamilton, G. F., "On the Flow of Water Induced by a Rising Column of Air Bubbles," in: International Association for Hydraulic Research, Proceedings of the Eighth Congress, Vol. 2, Montreal, 1959, Paper 7-D.
6. Kobus, H. E., "Analysis of the Flow Induced by Air Bubble Systems," Coastal Engineering Conference, Vol. II, Chapter 65, pp. 1016-1031, London, 1968.
7. Cederwall, K., and Ditmars, J. D., "Analysis of Air-Bubble Plumes". Report No. KH-R-24, W. M. Keck Laboratory of Hydraulics and Water Resources, Division of Engineering and Applied Science, California Institute of Technology, Pasadena, California, Sept. 1970.
8. Morton, B. R., Taylor, G. I., and Turner, J. S., "Turbulent Gravitational Convection from Maintained and Instantaneous Sources," Proc. of the Royal Society, Series A, vol. 234, pp. 1-23, 1956.
9. Balanin, V. V., Borokin, B. S., and Melkonyan, G. I., "Utilization of Deep Water Heat in Reservoirs for the Maintenance of Unfrozen Water Areas," Cold Regions Research and Engineering Laboratory, 1970 (Available as AD 716 306), Translation of a Russian report (1964).
10. Fand, R. M., and Keswani, K. K., "Mass Rate of Flow in the Natural-Convection Plume Above a Heated Horizontal Cylinder Immersed in a Liquid," Journal of Heat Transfer, Trans. ASME, Series C, Vol. 95, No. 2, May 1973, pp. 192-198.
11. Subramanian, G., and Tien, C., "Mixing in Liquid Phase Due to Bubble Motion," AIChE Paper No. 43D, 1970.
12. Morton, B. R., "Modeling Fire Plumes, "Proceedings of the Symposium (International) on Combustion, 10th, August 17-21, 1964 at University of Cambridge, Cambridge, England, 1965, pp. 973-982.
13. Ricou, F. P., and Spalding, D. B., "Measurements of Entrainment by Axisymmetrical Turbulent Jets, "Journal of Fluid Mechanics, Vol. 11, Pt. 1, Aug. 1961, pp. 21-32.
14. Scarborough, J. B., "Numerical Mathematical Analysis, "Fourth Ed., John Hopkins Press, Baltimore, 1958, pp. 314-322.
15. Zuber, N., and Findley, J. A., "Average Volumetric Concentration in Two-Phase Flow Systems," Journal of Heat Transfer, Trans. ASME, Series C, Vol. 87, No. 4, Nov. 1965, pp. 453-468.
16. Harmathy, T. Z., "Velocity of Large Drops and Bubbles in Media of Infinite or Restricted Extent," AIChE Journal, Vol. 6, No. 2, June 1960, pp. 281-288.
17. Weimer, J. C., Faeth, G. M., and Olson, D. R., "Penetration of Vapor Jets Submerged in Subcooled Liquids," AIChE Journal, Vol. 19, No. 3, May 1963, pp. 552-558.
18. Morton, B. R., "Forced Plumes," Journal of Fluid Mechanics, Vol. 5, Pt. 1, Jan. 1959, pp. 151-163.
19. Michel, B., Cold Regions Science and Engineering Monograph 3, Section B1a: "Winter Regime of Rivers and Lakes," U.S. Army Cold Regions Research and Engineering Laboratory, Report No. CCREL-CRSE-3-B1a, 1971. (Available as AD 724 121).

TABLE I. - VOLUMETRIC PUMPING RATES IN AN AXISYMMETRIC JET AT A LOCATION 3.3 M ABOVE ORIFICE SUBMERGED 4.5 M BELOW SURFACE

Air flow at standard conditions, Q_g, m^3/sec	Volume water pumped / Volume air = Q_l/Q_g			
	Kobus (6)	Baines (4) (extrapolated)	Present calculations $E_o = 0.08$	Present calculations $E_o = 0.116$
0.00040	175	349	217	327
.00130	100	236	108	163
.00255	86	188	73	110
.00420	67	159	54	81.5
.00620	62	140	42	63

TABLE II. - VOLUMETRIC PUMPING RATES FOR SUBMERGED AXISYMMETRIC JET OR PERFORATED PIPE (Q_g IS VOLUME FLOW AT ORIGIN OF GAS DISCHARGE)

Pipe depth, L	Q_g	Q_l/Q_g		Q_l/Q_g
m	m^3/sec	Axisymmetric jet, from eq. (17)		Perforated pipe 1 m long, eq. (19)
		$E_o = 0.08$	$E_o = 0.116$	
2	0.0001	284	440	717
	.001	71.4	111	154
	.01	17.9	27.8	33.3
3	0.0001	540	836	1090
	.001	136	211	234
	.01	34.1	52.8	50.6
6	0.0001	1490	2310	2250
	.001	374	580	485
	.01	94.0	146	105
12	0.0001	4460	6910	4720
	.001	1120	1740	1020
	.01	281	435	219